Thermal Bridging Calculation of Three Steel Stud Wall Assemblies with Benchmarking

M. Ghobadi[1] and J. Cingel[1]
[1] Façade Systems and Products, National Research Council Construction, Ottawa, ON, Canada

Introduction

The Pan-Canadian framework [1] on clean growth and climate change was adopted in December 2016 by the current Canadian government. The Pan-Canadian framework is a collective plan to grow the economy while reducing emissions and deploying measures to makes changes to the National Building Code that will help ensure building resilience when adapting to climate change. The federal government has an important role to play in both setting ambitious emission reduction targets and taking steps to achieve those goals. To support the 2030 target of reducing GHG emissions from federal operations by at least 40 per cent below 2005 levels, the 2017 budget proposed resources for NRCan to provide expertise to other federal departments for determining the best approaches to implement energy efficiency and clean energy technologies. Of Canada's total GHG emissions, 17% comes from homes and buildings whereas 12% are from direct emissions (e.g., combustion of natural gas for heating) and an additional 5% are emissions associated with electricity generation that is consumed in the built environment [1].

In this context, it is generally recognized that the thermal performance of building envelopes can be significantly affected by thermal bridging. Thermal bridges are localized areas of high heat flow through walls, roofs and other insulated building envelope components. Thermal bridging is caused by highly conductive elements that penetrate the thermal insulation or may also be caused by misaligned planes of thermal insulation. These paths allow heat flow to bypass the insulating layer thereby reducing the effectiveness of the insulation in providing resistance to heat loss to the building exterior.

In this project the COMSOL Multiphysics Heat Transfer Module was used to model the total thermal performance of three steel stud wall assemblies from which thermal bridging effects were calculated. Laboratory thermal tests were conducted on these wall assemblies in NRC's Guarded Hot Box test facility (GHB) following test procedures given in ASTM C1363 [2]. The results from thermal tests were used to benchmark the results derived from simulation. The benchmarking procedure demonstrated that the techniques and procedures used to produce R and RSI values can accurately reproduce test measurements using measured (or typical) material properties and consistent boundary conditions.

Experimental Set-up

Three walls were constructed for testing in the GHB. These wall assemblies each measured 2.44 m (96.0 in.) in height and 2.44 m (96.0 in.) in width. The depths of the three walls differed. Wall 1 (W1) was the narrowest wall assembly at 124 mm (4.875 in.) in depth; Wall 2 (W2) had a depth of 149 mm (5.875 in.), whereas; Wall 3 (W3) had the largest depth of wall assemblies tested of 175 mm (6.875 in.).

The basic wall construction shared by all three wall assemblies consisted of an interior gypsum drywall board, measuring 13 mm (0.5 in.) thick; 6 mm polyethylene vapour barrier; 20 gauge steel studs having a depth of 92 mm (3.625 in.) and 41 mm (1.625 in.) in width, and spaced 406 mm (16 in.) on centre; fiberglass batt R-12 insulation, 89 mm (3.50 in.) in depth; and an exterior layer of OSB sheathing measuring 16 mm (0.625 in.) in thickness. Wall assemblies W2 and W3 had an additional layer of XPS exterior insulation attached to the OSB sheathing. The insulation layers were 25 mm (1 in.) and 50 mm (2 in.) thick for W2 and W3 respectively. The wall assembly components are summarized in Table 1. Schematics of each wall assembly are presented in an exploded view in Figure 1 and Figure 2.

The NRC GHB test facility, for which a schematic is given in Figure 3, is a test apparatus specifically designed to determine the thermal resistance of building envelope assemblies and components by subjecting a test specimen to a temperature difference and measuring the amount of energy required to maintain interior set point conditions; i.e., the amount of heat the test specimen consumes to maintain the imposed temperature difference is measured and the thermal resistance is determined on the basis of the rate of heat transfer across the specimen, and as function of the unit area of the test specimen.

To determine the overall thermal resistance of the test specimen, measurements were taken of the interior (room-side) and exterior (weather-side) air temperature at the surface of the test specimen, as well as the heat input to the calorimeter thereby allowing the air temperature within the guard to be maintained to that of the room-side (interior) temperature. The thermal resistance can then be calculated using:

Table 1. Summary of three wall assembly components used in GHB tests

ID	Interior Sheathing	Fiberglass Cavity Insulation	Cavity Depth	Steel Stud Thickness	Steel Stud Spacing (o.c.)	Steel Stud Flange	Steel Track Thickness	Steel Track Flange	Exterior Sheathing	Exterior Insulation	Cladding
W1	1/2" (13 mm) gypsum	R-12 (RSI 2.1)	3-5/8" (92 mm)	20 gauge	16" (406 mm)	1 5/8" (41 mm)	1.03 mm	Not stated	5/8" (16 mm) OSB	none	none
W2	1/2" (13 mm) gypsum	R-12 (RSI 2.1)	3-5/8" (92 mm)	20 gauge	16" (406 mm)	1 5/8" (41 mm)	1.03 mm	Not stated	5/8" (16 mm) OSB	1" (25mm) XPS	none
W3	1/2" (13 mm) gypsum	R-12 (RSI 2.1)	3-5/8" (92 mm)	20 gauge	16" (406 mm)	1 5/8" (41 mm)	1.03 mm	Not stated	5/8" (16 mm) OSB	2" (50mm) XPS	none

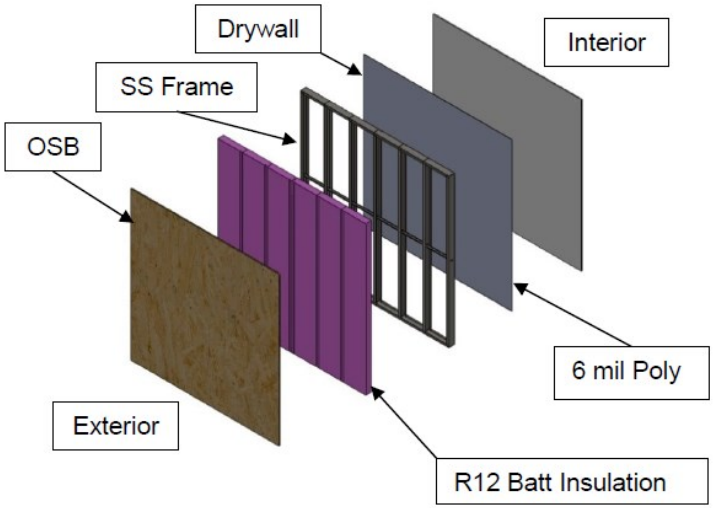

Figure 1. Schematic of wall assembly W1

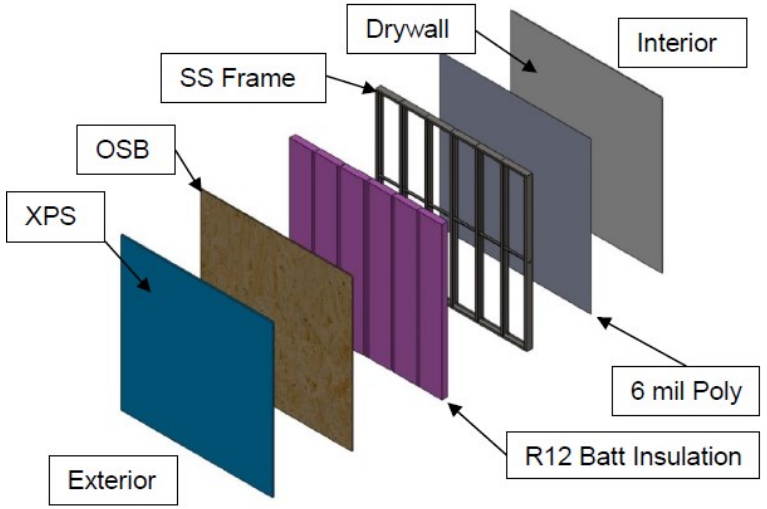

Figure 2. Schematic of wall assembly W2 and W3. Styrofoam (XPS – Extruded Polystyrene) panel was 25 mm (1 in.) thick for W2 & 50 mm (2 in.) thick for W3

Table 2. Exterior and interior boundary conditions

$T_{cold\ air}$ (°C)	$T_{hot\ air}$ (°C)	$T_{cold\ surface}$ (°C)	$T_{hot\ surface}$ (°C)	h_{cold} $(\frac{w}{m^2K})$	h_{hot} $(\frac{w}{m^2K})$
-5	21	-4.6818	19.824	32.7	9.2
-20	21	-19.513	19.19	34.0	8.9
-35	21	-34.355	18.589	34.0	8.9

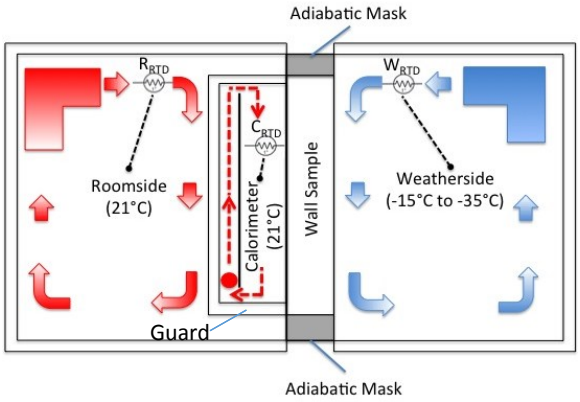

Figure 3. Schematic of GHB set-up & primary facility elements showing: room-side (interior) and weather-side (exterior) chambers, wall test specimen (sample), adiabatic mask, calorimeter and guard.

$$RSI = \frac{A*\Delta T}{Q}$$

Where:

Q = heat input to the calorimeter (W)

A = specimen area normal to the direction of heat transfer (m^2)

ΔT = absolute temperature difference between the interior and exterior air (°K)

In addition to the parameters mentioned previously, the interior and exterior surface temperatures of the wall assemblies were measured using thermocouples.

Numerical Simulation

Numerical simulations were completed on the wall assemblies in three dimensions. The modeling sequence for both series consisted of: (i) selecting and creating the geometry to be modelled; (ii) selecting the material properties; (iii) determining and applying the boundary conditions; (iv) performing mesh verification; (v) conducting the numerical simulations, and; (vi) comparing the results to those obtained from laboratory tests.

The 3-D geometries for the wall assemblies were created in Solidworks®. The geometries were imported in COMSOL Multiphysics and material properties were assigned to the corresponding domains. The temperature dependent thermal conductivity was used for fiberglass insulation batt and extruded polystyrene (XPS) as follow:

$K_{Fibergalss} = 0.03438+0.000212T_{mean}$

$K_{XPS} = 0.0271+0.0001129T_{mean}$

Three different boundary conditions were applied on the wall assemblies. The temperatures and convective heat transfer coefficients used for the two sides of the wall assemblies are shown in Table 2. A parametric sweep of the cold side temperature was conducted for these simulations. The average surface temperatures and the total heat flux passing through wall were measured and the thermal resistance was calculated using the correlation stated in the experimental section.

Contact thermal resistances were also considered in modelling the wall assemblies that were tested. The 2009 ASHRAE Handbook – Fundamentals [3] states that the contact resistances in buildings are too small to be of concern in many cases, but might be important for steel framing. Furthermore, contact resistance has previously been shown to be important for accurately simulating the thermal performance of steel stud assemblies [4]. To better model the thermal performance of the wall assemblies, contact resistances were also considered when undertaking simulations. For these purposes a value for contact resistance of 0.057 $hr.ft^2.{}^oF/Btu$ (0.010 $m^2\,{}^oC/W$) was modeled at insulation interfaces, whereas a value of 0.011 $hr.ft^2.{}^oF/Btu$ (0.0020 $m^2\,{}^oC/W$) was used in the model configuration at steel to steel connections.

Results

The wall assemblies that were described before were tested in the NRC GHB facility. The results were used to benchmark the COMSOL simulations. Surface to surface (S-t-S) R values were measured and compared for three outdoor temperatures: -5 °C, -20 °C and -35 °C.

The S-t-S R and RSI values derived from COMOSL for wall assemblies W1, W2, and W3 are provided, respectively, in **Error! Reference source not found.**. These have been benchmarked against the GHB results. For W1, an outdoor temperature of -35 °C could not be achieved in the cold side of GHB because the calorimeter heater could not compensate for the heat flow through the wall and the mask at that temperature. It can be seen that the difference between the calculated R values for W1 is 4.34% on average which is below the ± 8% uncertainty reported for the NRC GHB. The average difference is 1.42% for W2 and 4.80% for W3.

The effect of thermal bridging has also been studied numerically. The R-values were calculated for the WAs supposing the steel studs had been replaced with the glass-fiber insulation from which the increase in R-value was then calculated. Average increases in R-value were found to be 115% for W1, 61% for W2 and 38% for W3. It can be seen that the effect of thermal bridging becomes less significant by applying additional exterior insulation to the WA. To normalize the temperature results for different outside temperatures, temperatures are non-dimensionalized using the temperature index approach. The temperature index is the ratio of a surface temperature to the overall temperature difference between indoor and outdoor. A value of 0 is the outdoor air temperature and 1 is the indoor air temperature.

Table 3. Benchmarking results for Wall 1, Wall 2 and Wall 3

	COMSOL results		GHB Results			No Thermal Bridging		
T_o (°C)	RSI S-t-S	R S-t-S	RSI S-t-S	R S-t-S	Difference	RSI S-t-S	R S-t-S	Increase
Wall 1								
-5	1.36	7.77	1.43	8.17	**5.13%**	2.82	16.02	**106%**
-20	1.37	7.73	1.42	8.30	**3.55%**	3.03	17.20	**122%**
-35	1.45	8.14				3.14	17.82	**119%**
Wall 2								
-5	2.26	12.86	2.35	13.34	**3.66%**	3.59	20.40	**59%**
-20	2.39	13.60	2.40	13.63	**0.21%**	3.87	21.96	**61%**
-35	2.46	13.97	2.45	13.91	**0.39%**	3.98	22.59	**62%**
Wall 3								
-5	3.27	18.57	3.15	17.89	**3.84%**	4.62	26.22	**41%**
-20	3.37	19.14	3.23	18.34	**4.37%**	4.89	27.77	**45%**
-35	3.43	19.48	3.23	18.34	**6.21%**	5.02	28.51	**46%**

$$T_i = \frac{T_{surface} - T_{outdoor}}{T_{indoor} - T_{outdoor}}$$

Temperature index contours for the interior and exterior of the wall assemblies along with minimum and maximum values of temperature indices on the surfaces are depicted in Figure 4, Figure 5 and Figure 6 respectively for W1, W2 and W3. The temperature variation can be seen on both exterior and interior surfaces on W1 where no exterior insulation is used. The temperature variation on the exterior surface becomes less significant by adding exterior insulation. The effects become less visible on the interior surface but still can be observed from the temperature index contours. The temperature index difference on the interior side is 0.22 for W1, 0.08 for W2 and 0.07 for W3.

Figure 8 illustrates the temperature index on the warm surface along a steel stud for W3. It can be seen that the temperature index drops from 0.982 to 0.928 on the stud because of the higher conductivity of the steel in comparison to air. Figure 9Figure 3 shows the temperature index at a cross section of W3 and in Figure 9 isothermal surfaces are illustrated at the cross section along two studs. The thermal bridging effect of steel studs through which heat is conducted can readily be observed.

Conclusions

This project consisted in conducting Guarded Hot Box (GHB) tests and COMSOL Multiphysics simulations. Three wall assemblies were fabricated and tested in the NRC GHB. The results from the tests were used to benchmark the results derived from numerical simulations. Different outdoor temperatures were also studied to reflect different climate zones in Canada.

- Three steel stud wall assemblies tested in NRC's GHB test facilities and another series of simulations were conducted and benchmarked against these results. Average differences of 4.34%, 1.42% and 4.80% were observed between numerical results obtained in this study and the reported GHB results.
- Another series of simulations was also conducted in which the thermal bridging material (steel) was replaced with the embedded insulation (glass-fiber) and the R value calculated. Average R value increases of 115%, 61% and 38% were obtained for the wall assemblies considered. It has been shown that the effects of thermal bridging become less important by adding exterior insulation.
- It has also been shown that using highly conductive materials together with typical insulation materials can significantly decrease the thermal performance of wall assemblies.

This is an ongoing project and additional wall assemblies have been or will be tested and benchmarked against results obtained from numerical simulation. This project has demonstrated that the results derived from the COMSOL Multiphysics software is capable of predicting the thermal performance of steel stud wall assemblies with a high precision.

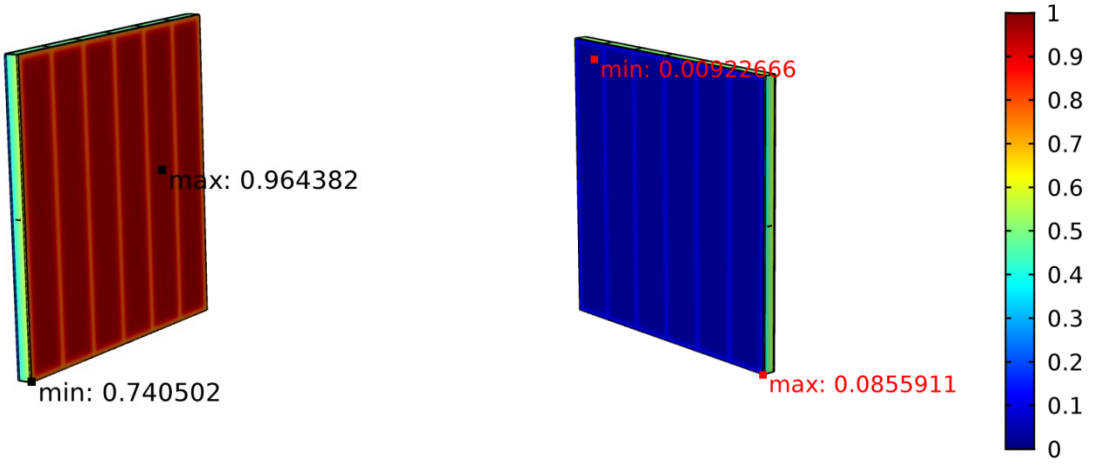

Figure 4: W1 - Values of temperature index on the Interior surface (left) and exterior surface (right) of WA

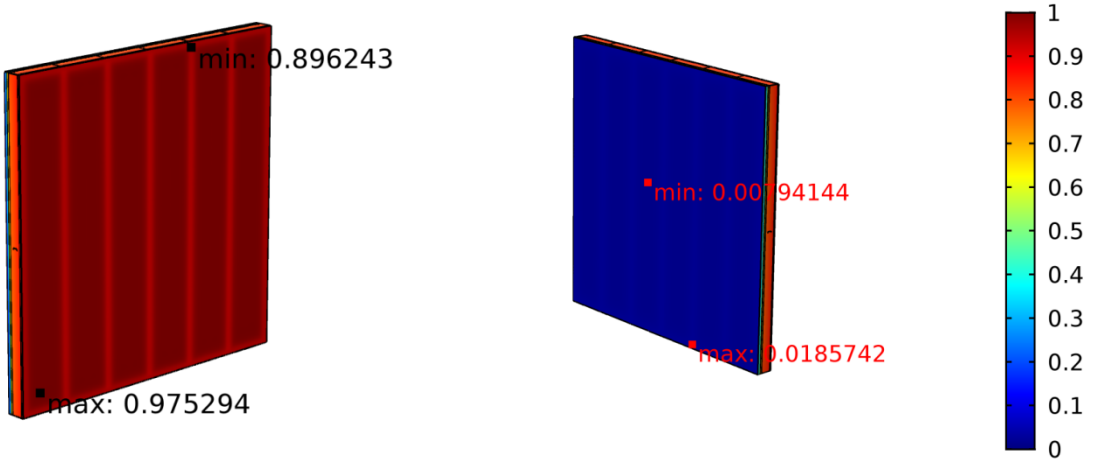

Figure 5: Interior surface (left) and exterior surface (right) temperature index for W2

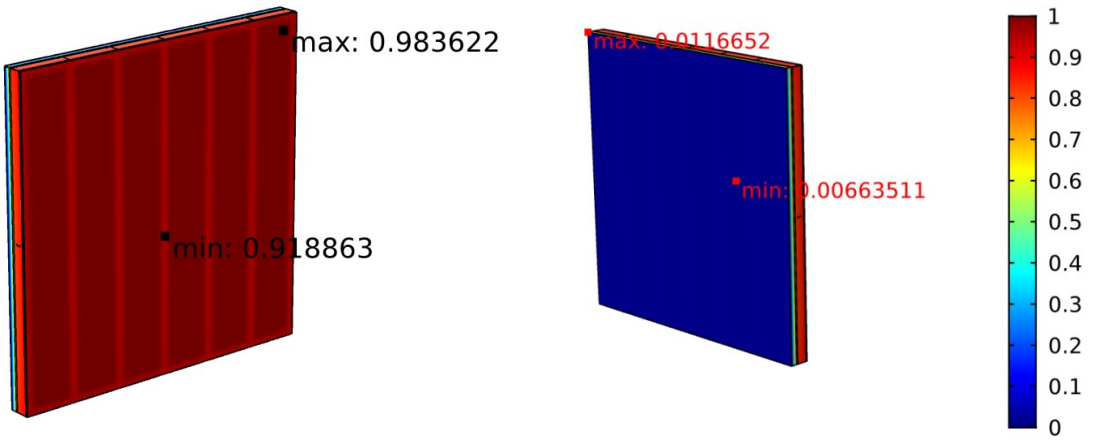

Figure 6: Interior surface (left) and exterior surface (right) temperature index for W3

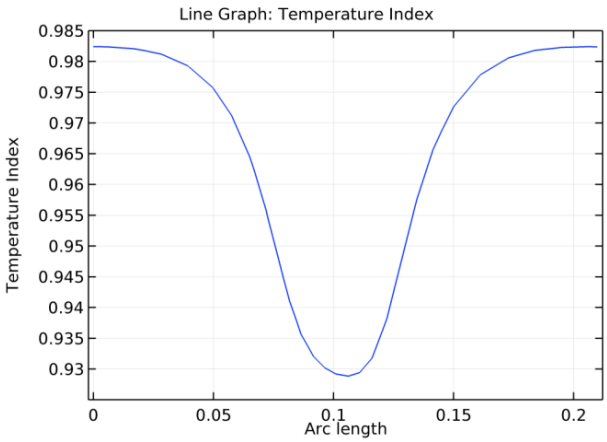

Figure 7. Temperature along a stud on the warm surface for W3

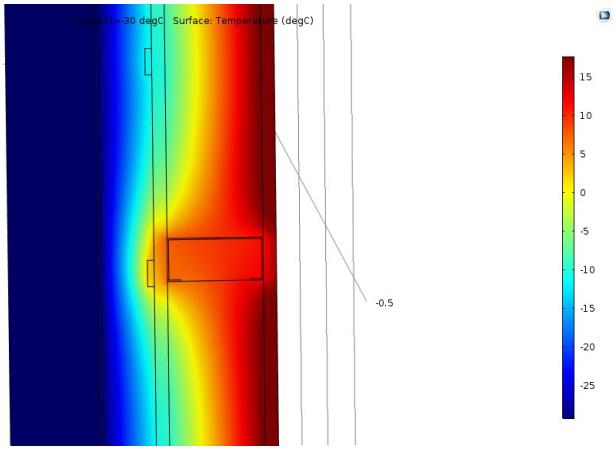

Figure 8. Temperature index at the cross section (right) along steel studs for W3

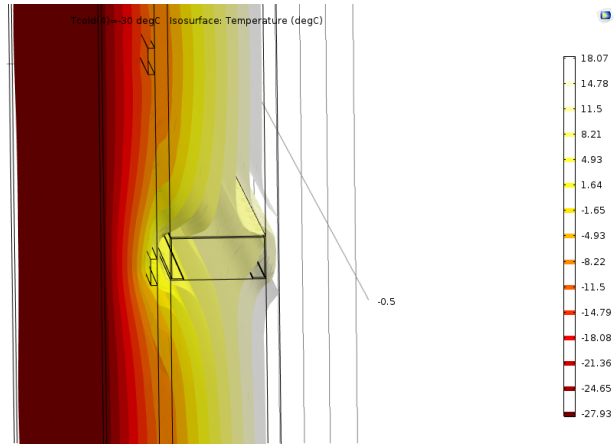

Figure 9. Isothermal surfaces at a cross section for W3

References

1. *Pan-Canadian Framework on Clean Growth and Climate Change – Environment and Climate Change Canada, 2016.*
2. *Thermal Performance of Building Envelope Details for Mid- and High-Rise Buildings (1365-RP) (2011), Presented to Technical Committee 4.4, Building Materials and Building Envelope Performance of ASHRAE, Report No. 5085243.01.*
3. *Building Envelope Thermal Bridging Guide – Version 1.1 (2016), BC Hydro.*
4. *ASTM C1363 – 11 Standard Test Method for Thermal Performance of Building Materials and Envelope Assemblies by Means of a Hot Box Apparatus*

Acknowledgements

The authors acknowledge the financial support of NRCan to support the Net Zero Thermal Bridging project.